Intermetallic Compound Pd_2Ga as a Selective Catalyst for the Semi-Hydrogenation of Acetylene: From Model to High Performance Systems†

Antje Ota,‡ Marc Armbrüster,*,§ Malte Behrens,*,‡ Dirk Rosenthal,‡ Matthias Friedrich,§ Igor Kasatkin,‡ Frank Girgsdies,‡ Wei Zhang,‡ Ronald Wagner,‡ and Robert Schlögl‡

Fritz-Haber-Institute of Max-Planck-Society, Department of Inorganic Chemistry, Faradayweg 4-6, 14195 Berlin, Germany, and Max-Planck-Institut für Chemische Physik fester Stoffe, Nöthnitzer Straβe 40, 01187 Dresden, Germany

Received: September 27, 2010; Revised Manuscript Received: November 29, 2010

A novel nanostructured Pd_2Ga intermetallic catalyst is presented and compared to elemental Pd and a macroscopic bulk Pd_2Ga material concerning physical and chemical properties. The new material was prepared by controlled coprecipitation from a single phase layered double hydroxide precursor or hydrotalcite-like compound, of the composition $Pd_{0.025}Mg_{0.675}Ga_{0.3}(OH)_2(CO_3)_{0.15}\cdot mH_2O$. Upon thermal reduction in hydrogen, bimetallic nanoparticles of an average size less than 10 nm and a porous $MgO/MgGa_2O_4$ support were formed. HRTEM images confirmed the presence of the intermetallic compound Pd_2Ga and are corroborated by XPS investigations which revealed an interaction between Pd and Ga. Due to the relatively high dispersion of the intermetallic compound, the catalytic activity of the sample in the semihydrogenation of acetylene was more than 5000 times higher than observed for a bulk Pd_2Ga model catalyst. Interestingly, the high selectivity of the model catalyst toward the semihydrogenated product of 74% was only slightly lowered to 70% for the nanostructured catalyst, while an elemental Pd reference catalyst showed only a selectivity of around 20% under these testing conditions. This result indicates the structural integrity of the intermetallic compound and the absence of elemental Pd in the nanosized particles. Thus, this work serves as an example of how the unique properties of an intermetallic compound, well-studied as a model catalyst, can be made accessible as real high-performing material allowing establishment of structure−performance relationships and other application-related investigations. The general synthesis approach is assumed to be applicable to several Pd−X intermetallic catalysts, with X being elements forming hydrotalcite-like precursors in their ionic form.

Introduction

Pd is a highly active noble metal catalyst for hydrogenation reactions,[1,2] e.g., the hydrogenation of acetylene. Among the Pd-based catalysts, Pd−Ag alloy catalysts show a higher selectivity toward the semihydrogenated product, ethylene, than pure Pd catalysts, which favor total hydrogenation to ethane, and are the currently industrially employed system for this process.[3] The modification of the electronic, adsorptive, and catalytic properties of Pd-based catalysts by the presence of a second species has recently received considerable attention. Calculations of the potential energy diagram for the hydrogenation of acetylene over pure Pd and Pd−Ag have shown that the addition of Ag lowers the energy barrier of desorption of the intermediately formed ethylene with respect to the energy barrier of further hydrogenation to ethane and thus makes the catalyst more selective.[4] Similar effects are also predicted for other modifying atoms in the subsurface of Pd.[5] It was shown experimentally that conditions of selective alkyne hydrogenation can also be found if pure Pd metal is used as starting material. In situ investigations have shown that under these conditions in fact a Pd−C phase is in operation,[6] which was formed by fragmentation of the reactant molecule and migration of carbon into the subsurface.[7] Among the Pd−X materials investigated as hydrogenation catalysts, bulk Pd−Ga intermetallic compounds (IMCs) have shown extraordinarily high selectivities and stability in the semihydrogenation of acetylene.[8] IMCs are single-phase materials which consist of two or more metallic elements. In contrast to alloys, they adopt an ordered crystal structure different from those of the constituting metals themselves.[8,9] Thus, also their chemical properties may differ substantially, and they should be considered as a class of materials in their own right, requiring an independent physicochemical characterization. This has recently been demonstrated for the structurally ordered IMCs PdGa and Pd_3Ga_7.[10,11] The in situ stability of these IMCs in reaction atmosphere and the important suppression of hydride formation were attributed to the presence of an ordered and partially covalent bonding network between Pd and Ga in contrast to statistically arranged substitutional alloys. Unfortunately, as for most other Pd−X systems, homogeneous and nanostructured versions of Pd−Ga IMCs allowing a transfer of theoretically predicted properties or of the results already confirmed for macroscopic model systems to "real" catalysts are hard to obtain.

The general procedure to synthesize Pd−Ga IMCs is by melting the appropriate amounts of the elements followed by annealing at high temperatures in inert atmosphere. This direct reaction leads to well-defined and phase-pure model materials, which are very useful to study the intrinsic catalytic properties of IMCs. The material obtained is in thermodynamic equilibrium, easing the reproducible synthesis. Top-down approaches,

† Part of the "Alfons Baiker Festschrift".

* Corresponding authors. E-mail: research@armbruester.net. Tel.: +49 351 46 46 22 31. Fax: +49 351 46 46 40 01 (MA). E-mail: behrens@fhi-berlin.mpg.de. Tel.: +49 30 8413-4408. Fax: +49 30 8413-4405 (MB).

‡ Fritz-Haber-Institute of Max Planck Society.

§ Max-Planck-Institut für Chemische Physik fester Stoffe.

10.1021/jp109226r
Published on Web 12/10/2010

e.g., milling or etching of bulk intermetallic compounds,[12] lead to an increase in surface area but go hand in hand with a partial destruction of the IMC crystal structure, not only being detrimental for the catalytic selectivity but also complicating the establishment of structure−performance relationships. Thus, to check if the unique structural and catalytic properties of bulk IMCs can be maintained or even extrapolated from the world of model catalysis to real systems, i.e., over several orders of magnitude in particle size, bottom-up approaches are necessary.

One possibility to prepare supported and dispersed IMCs is by reaction between noble metal and the oxide support. An example is the formation of Pd−Ga intermetallic compounds by reductive treatment at elevated temperatures of Pd/Ga_2O_3.[13−15] Single-phase and nanosized Pd−Ga intermetallic compounds can be synthesized by coreduction of $GaCl_3$ and $Pd(acac)_2$ in THF by Superhydride.[16] This synthesis leads to very small particles of the intermetallic compounds and surface areas of more than 2 m^2/g. Applied as catalysts, these materials were shown to keep the high intrinsic selectivity of the Pd−Ga IMCs, while the specific activity is increased by a factor of up to 32 000. However, this method of preparation necessitates expensive reactants as well as inert atmosphere during the synthesis process, making it ineligible for industrial application.

Herein, we present a novel nanosized IMC catalyst prepared by a more feasible synthetic approach using a hydrotalcite-based material as precursor for supported Pd−Ga IMCs and address the question if the unique structural and electronic properties found in this system also persist in the form of nanoparticles enabling interesting catalytic performance. Hydrotalcite-like compounds (HTlc's) are easily accessible by coprecipitation from aqueous solutions and represent well-established precursor systems[17] for bulk catalysts, applied, e.g., in preparation of Ni−Al steam reforming[18] or Cu−Zn−Al methanol synthesis catalysts.[19] HTlc's exhibit the general composition $(M1^{II},M2^{II})_{1-x}M3^{III}_x(OH)_2(CO_3)_{x/2}\cdot mH_2O$ ($0.25 \le x \le 0.33$) and a layered structure, in which all metal cations are uniformly distributed in slabs of edge-sharing MO_6 octahedra. HTlc precursors thus present well-defined and homogeneous starting materials for the preparation of supported IMCs.

The final $Pd_2Ga/MgO/MgGa_2O_4$ catalyst obtained by the HTlc precursor approach described above was characterized using nitrogen physisorption, XRD, HRTEM, and XPS. To investigate possible particle size effects in this system, the structural, electronic, and catalytic properties in the semihydrogenation of acetylene are compared to those of elemental Pd and those of the unsupported bulk counterpart, a Pd_2Ga catalyst prepared by direct reaction of the elements as described in refs 10 and 11.

Experimental Section

Synthesis Procedures. The PdMgGa HTlc precursor (atomic ratio 2.5:67.5:30) was synthesized by controlled coprecipitation at pH = 8.5 and 55 °C by cofeeding appropriate amounts of mixed aqueous metal nitrate ($[Pd^{2+}] + [Mg^{2+}] + [Ga^{3+}] = 0.2$ M) and 0.345 M sodium carbonate solution as the precipitating agent. Both solutions were added simultaneously dropwise into a 2 L precipitation reactor (Mettler-Toledo LabMax). The nitrate solution was automatically pumped with a constant dosing rate, and the basic solution was added to maintain a constant pH of 8.5. After completion of addition, the mixture was stirred for 1 h at 55 °C. The precipitate was filtered and washed twice with warm deionized water (55 °C) to remove all nitrate and sodium ions. The obtained conductivity of the filtrate was lower than 0.5 mS/cm, and no sodium contamination could be detected by EDX. The solid was dried for 12 h at 80 °C in air. The precursor was reduced in 5% H_2 in argon at 550 °C to obtain the supported Pd−Ga intermetallic compound. The heating rate was 2 °C/min, and the final temperature was kept for 4 h.

A second catalyst, consisting of bulk Pd_2Ga, was prepared for reference purposes by melting Pd (ChemPur 99.95%) and Ga (ChemPur 99.99%) in a 2:1 molar ratio in glassy carbon crucibles under an argon atmosphere in a high-frequency induction furnace. After the exothermic reaction of the metals, the product was cooled to ambient temperature, enclosed in an evacuated quartz glass ampule, and annealed at 900 °C for 100 h. Subsequently, the samples were quenched in water, and the phase purity was verified by transmission powder X-ray diffraction.

Characterization Techniques. ***Electron Microscopy.*** For TEM investigations, a Philips CM200FEG microscope operated at 200 kV and equipped with a field emission gun, the Gatan imaging filter, and energy-dispersive X-ray (EDX) analyzer was used. The coefficient of spherical aberration was $C_s = 1.35$ mm, and the information limit was better than 0.18 nm. High-resolution images with a pixel size of 0.016 nm were taken at the magnification of 1 083 000 with a CCD camera, and selected areas were processed to obtain the power spectra (square of the Fourier transform of the image), which were used for measuring interplanar distances (±0.5%) and angles (±0.5°) for phase identification. Scanning electron microscopy was employed for investigation of particle morphology and metal distribution of the HTlc precursor using a Hitachi S-4800 (FEG) system.

X-ray Diffraction. XRD measurements of the Pd_2Ga sample obtained by the direct reaction between the metals were performed on an image plate Guinier camera (G670, Huber, Cu $K\alpha_1$ radiation, $\lambda = 1.54056$ Å, quartz monochromator, $3° \le 2\theta \le 100°$) in transmission mode. For the measurements, the finely powdered sample was mounted with the aid of Vaseline on a 3 μm Kapton foil. For the ex-HTlc samples the measurements were performed in Bragg−Brentano reflection geometry on a Bruker AXS D8 Advance diffractometer equipped with a secondary graphite monochromator (Cu $K\alpha$ radiation) and scintillation detector. The sample powder was filled into the flat circular recess of a sample holder which was sealed with an airtight X-ray transparent dome to avoid prolonged air contact. XRD patterns of the HTlc precursor and its decomposition products were recorded on a STOE Stadi P diffractometer in transmission geometry using Cu $K\alpha_1$ radiation, a primary Ge monochromator, and a 3° linear position sensitive detector.

X-ray Photoemission Spectroscopy. All XP spectra were recorded with fixed analyzer transmission at room temperature, using nonmonochromatized Mg $K\alpha$ radiation at a pass energy of 20 eV leading to fwhm < 1.1 eV of Ag $3d_{5/2}$. The binding energy scale of the system was calibrated using Au $4f_{7/2} = 84.0$ eV and Cu $2p_{3/2} = 932.7$ eV from foil samples. The angle between the sample normal and the analyzer was 30° and between the X-ray gun and the sample normal 54°. Deconvolution of the spectra was conducted by 70/30 G-Lorentz product functions after subtraction of a Shirley background. To avoid contamination or oxidations on the surface, the catalyst pellet was prereduced at 550 °C in diluted hydrogen (5%) for 4 h to have the as-synthesized state prior to the measurement and transferred to the XPS chamber without air contact.

Specific Surface Area Determination. Specific surface areas of the precursors and the reduced samples were determined by N_2 physisorption in an Autosorb-1C setup (Quantachrome) using the BET method. Prior to the measurements, 30 mg of the

samples was degassed for 2 h at 80 °C for the precursors and at 150 °C for the reduced samples, respectively.

Chemical Analysis. About 5 mg of sample was exactly weighed and dissolved in 2 mL of aqua regia. The solutions were transferred to and filled up 50 mL volumetric flasks. The content of the metals was determined with ICP-OES (Vista RL, Varian) after matrix-matched calibration.

Catalytic Measurements. Catalytic investigations were performed in a quartz glass plug flow reactor with an inner diameter of 7 mm. The catalyst bed was supported by a quartz glass frit and consisted of the stated sample amounts diluted in 150 mg of catalytically inert boron nitride (hexagonal, 99.5%, 325 mesh, Aldrich) to improve the flow characteristics. No pressure drop was observed at a total gas flow of 30 mL/min. In the case of the directly synthesized Pd_2Ga, the samples were comminuted in an agate mortar in inert atmosphere prior to the catalytic measurements resulting in particle sizes below 20 μm. In the case of the HTlc approach, the precursor (0.4−1 μm) was reduced in situ (5% H_2, 4 h, 500 °C). The reactant mixture consisted of 0.5% C_2H_2 (premixed 5% C_2H_2, 99.6% in He, 99.996%), 5% H_2 (99.999%), and 50% C_2H_4 (99.95%) in helium (99.999%). All gases except ethylene (Westfalen Gas) were obtained by Praxair. Gases were mixed using Bronkhorst mass flow controllers. Reactant and product composition were analyzed with a Varian CP 4900 micro gas chromatograph. Conversion of acetylene and selectivity to ethylene were calculated as

$$X_{C_2H_2} = \frac{c_{feed} - c_x}{c_{feed}} \times 100\%$$

and

$$S_{C_2H_4} = \frac{c_{C_2H_4}}{c_{C_2H_4} + c_{C_2H_6} + 2c_{C_4H_x}} = \frac{X_{C_2H_2}}{X_{C_2H_2} + c_{C_2H_6} + 2c_{C_4H_x}} = \frac{(c_{C_2H_2,feed} - c_{C_2H_2,product})}{(c_{C_2H_2,feed} - c_{C_2H_2,product}) + c_{C_2H_6} + 2c_{C_4H_x}}$$

where c_{feed} represents the acetylene concentration in the feed and c_x is the acetylene concentration in the product. It is assumed that acetylene is only hydrogenated to ethylene, which may be further hydrogenated to ethane. Higher hydrocarbons than C4 were not observed in the experiments. The reaction temperature was 200 °C. The other conditions were chosen to be comparable to those reported in refs 10 and 11.

Results and Discussion

It is noted that Pd^{2+} is not easily incorporated in the HTlc layers due to its larger ionic size compared to Mg^{2+}, which exceeds the empirical limit of approximately 0.80 Å for the incorporation into a HTlc.[20] Furthermore, Pd^{2+} exhibits a tendency toward 4-fold square-planar coordination in aqueous solutions instead of an octahedral one present in HTlc. Therefore, only small amounts of Pd^{2+} could be incorporated in the HTlc precursor, and a second bivalent cation is required to achieve crystallization of all Pd ions in a single HTlc phase. In our example, we have chosen $M2^{II} = Mg^{2+}$ to not interfere with the redox chemistry of the Pd−Ga system. The relative amount of trivalent cations in HTlc ranges from approximately 1:4 to 1:3, and the value of x was set to 0.3 in our preparation. Mg as well as residual Ga will remain in their oxidized states and form the support material for the Pd−Ga IMC nanoparticles. Thus, due to the homogeneous distribution and the low amount of Pd in the HTlc precursor, the formation of very small and reactive Pd^0 particles is expected upon initial reduction, and the interaction with the surrounding Ga^{3+}−oxide matrix is assumed to be maximized. Clearly, the challenging step is the unfavorable reduction of Ga^{3+}, which requires elevated temperatures and competes with phase segregation and sintering. The single-phase HTlc precursor is expected to favor the formation of homogeneous, single-phased, and nanosized Pd−Ga IMCs because it provides a homogeneous microstructure concerning Pd particle size and Pd metal−oxide interactions. The Ga reduction is likely to be triggered by the strong reducing power of atomic spillover hydrogen formed on the initially formed embedded Pd^0 particles.[21] An additional advantage of the HTlc precursor method is that the synthesis is based on conventional aqueous coprecipitation which allows a feasible up-scaling.

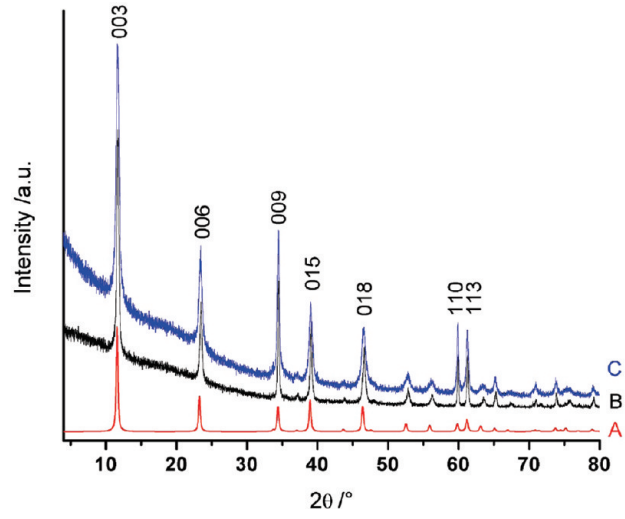

Figure 1. (A) Simulated XRD pattern of MgGa HTlc. (B) XRD pattern of undoped MgGa HTlc precursor. (C) Pd-doped MgGa HTlc precursor.

TABLE 1: XRD Results of the HTl Precursors

	lattice parameter		fwhm	
sample	a (Å)	c (Å)	d_{003} (°2θ)	d_{110} (°2θ)
$Mg_{0.66}Ga_{0.34}$	3.09	22.74	0.29	0.18
$Mg_{0.63}Ga_{0.34}Pd_{0.03}$	3.09	22.78	0.49	0.26

Figure 1 shows the XRD pattern of a Pd-doped HTlc precursor (2.5 mol % Pd, i.e., $Pd_{0.025}Mg_{0.675}Ga_{0.3}(OH)_2(CO_3)_{0.15}\cdot mH_2O$, corresponding to 3.21 wt % Pd) in comparison with the undoped pure MgGa HTlc, $Mg_{0.7}Ga_{0.3}(OH)_2(CO_3)_{0.15}\cdot mH_2O$. Both materials crystallize in the HTlc structure and exhibit high crystallinity. No other crystalline phases could be detected by XRD. The Pd content was determined to 2.83 wt % in the precursor by ICP-OES, from which a water content of $m = 0.66$ results, in accordance with ref 22. Due to the low total amount of Pd, the lattice parameters of the HTlc precursors change only slightly (Table 1). As expected for HTlc, the particle morphology is platelet-like, and the homogeneous distribution of Pd within the platelets is evidenced by elemental mapping of the precursor in the SEM (Figure 2). No Pd-rich aggregates of Pd oxide or hydroxide could be detected. The specific surface area increased from 45 m^2/g to 67 m^2/g by substitution of 2.5%

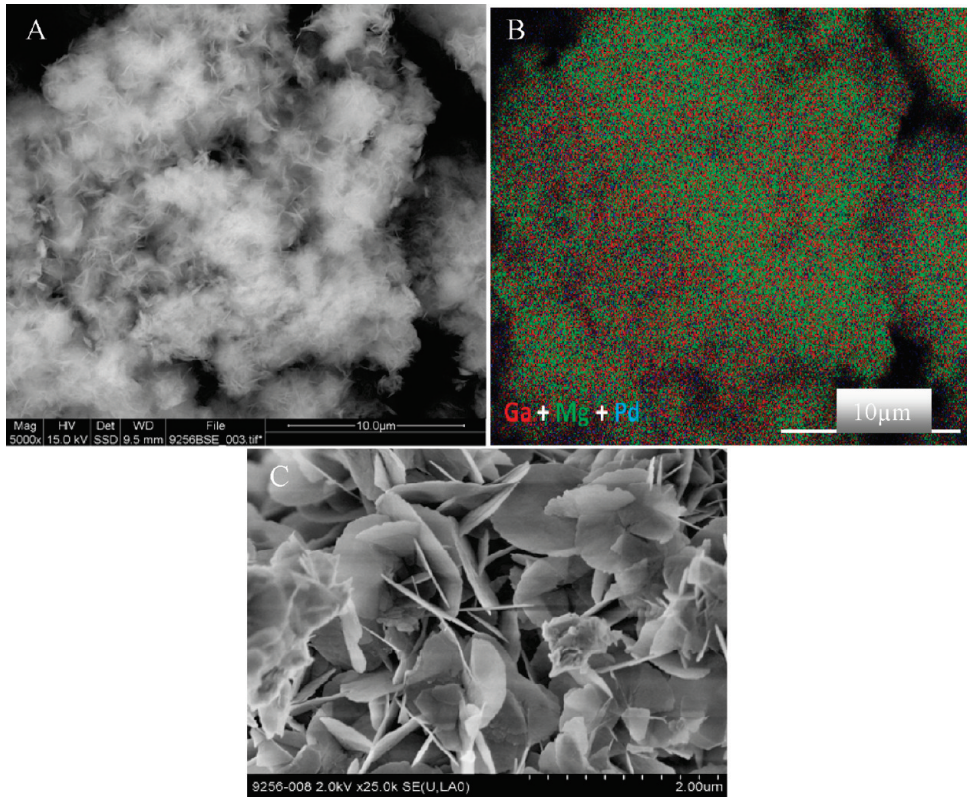

Figure 2. Morphological characterization and elemental mapping of the 2.5 mol % Pd-doped HTlc precursor. A: Low magnification SEM image. B: Corresponding elemental mapping. C: Particle morphology at higher magnification.

Mg by Pd probably due to hindered crystallite growth in the Pd-distorted HTlc. This assumption is supported by significantly higher fwhm values of the HTlc material, corresponding to smaller crystallites, in the case of the Pd-doped precursor (Table 1). The particle size of the HTlc platelets is in the range of 0.4−1 μm, according to SEM (Figure 2c). To obtain the IMC, the reduction of the crystalline precursor was performed without prior calcination in diluted hydrogen at 550 °C. The reduction enhanced the porosity of the material, and an increased surface area of 109 m^2/g was measured for the Pd-doped sample after reduction. By taking into account the weight loss of water and carbon dioxide during thermal reduction, the Pd content of the reduced material is calculated to 4.49 wt %. The HTlc structure was destroyed by the thermal treatment, and only broad modulations assigned to poorly crystalline MgO and $MgGa_2O_4$ spinel (Figure 3) could be detected by XRD. In particular, no crystalline Pd phase could be unambiguously identified after thermal treatment. This is most probably a crystallite size effect caused by the high dispersion and low total amount of the Pd-containing phase. Using HRTEM, however, spherical and faceted particles of the IMC Pd_2Ga were identified after reduction of the precursor (Figure 4). In agreement with XRD, the crystalline fraction of the oxidic support was identified as $MgGa_2O_4$ spinel, which has maintained the platelet-like morphology. No particles of elemental Pd or other Pd−Ga IMCs than Pd_2Ga were detected by HRTEM even after careful investigation, supporting the homogeneity of the supported $Pd_2Ga/MgO/MgGa_2O_4$ catalyst. The mean particle diameter of the supported Pd_2Ga sample was determined from projected areas measured for 882 particles in several representative images and amounts to 6.7 ± 0.1 nm (standard deviation). The particle size distribution ranges from 1 to 30 nm for individual particles (Figure 4, inset) and the volume-weighted mean size is 8.6 nm.

To get more integral information on the Pd_2Ga phase, the surface of the catalyst was investigated by XPS after a pretreatment in hydrogen and without exposure to air. The sample shows strong charging during XPS measurements. After several hours, the peak positions remain constant. All signals are shifted by 5.5 eV referenced to the strongest carbon 1s signal at 285.0 eV. This results in a binding energy for Mg $2p_{3/2}$ of 50.2 eV. The $Ga2p_{3/2}$ peak exhibited a binding energy of 1118.8 eV for the oxidic gallium but also a small component at 1116.1 eV which is in a good agreement with metallic Ga (1116.3 eV[23]). The Pd $3d_{5/2}$ signal at 336.1 eV is shifted to higher binding energies compared to metallic Pd (Figure 5) and almost symmetric. In comparison to the bulk Pd_2Ga phase, the measured $Pd3d_{5/2}$ binding energy of the ex-HTlc catalyst is slightly higher.[24] This could be a size effect since for small particles

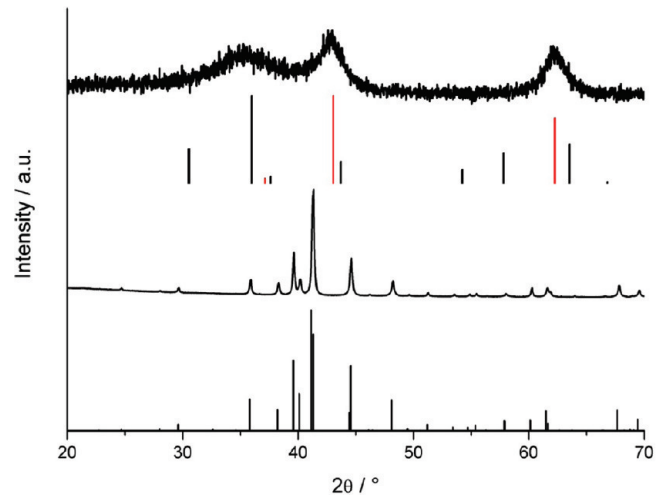

Figure 3. (a) XRD patterns of the catalyst obtained by reduction of the Pd-doped HTlc precursor. (b) ICDD 10-113 $MgGa_2O_4$ (black); ICDD 1-1235 MgO (red). (c) Bulk Pd_2Ga obtained by direct synthesis. (d) Pd_2Ga.[30]

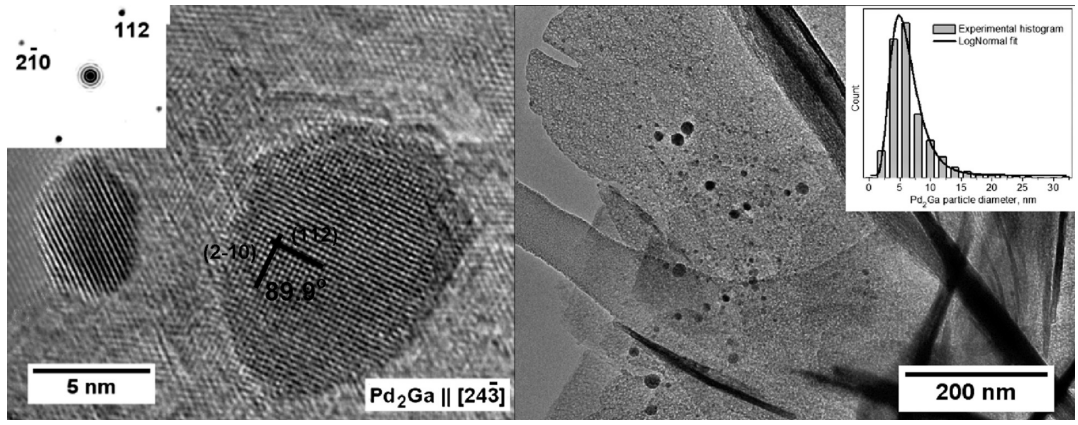

Figure 4. HRTEM images of $Pd_2Ga/MgO/MgGa_2O_4$ after reduction at 550 °C in 5% H_2/Ar. Inset in the left image shows a Fourier transform of the larger particle; the zone axis direction is indicated in the image. Inset in the right image shows the particle size frequency distribution histogram fitted with a log-normal curve.

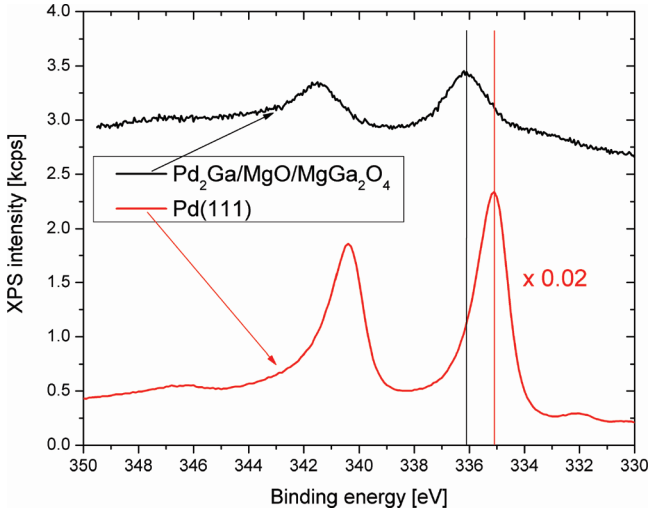

Figure 5. XPS data of the Pd 3d peaks of the nanostructured $Pd_2Ga/MgO/MgGa_2O_4$ catalyst compared with metallic Pd.

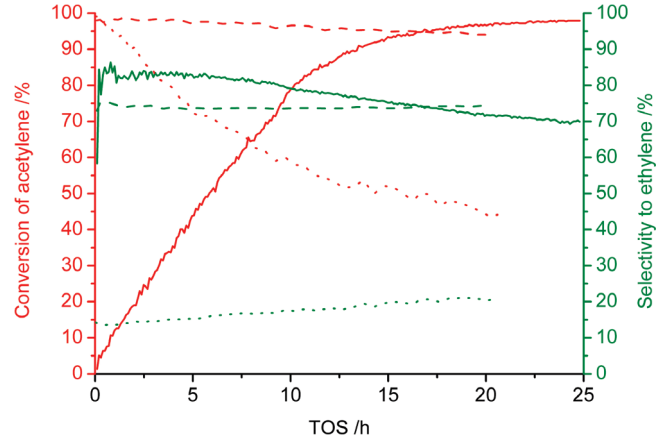

Figure 6. Catalytic properties of $Pd_2Ga/MgO/MgGa_2O_4$ (solid line), bulk Pd_2Ga (dashed line), and 5 wt % Pd/Al_2O_3 (Aldrich; dotted line).

the positive charge of the core hole will be screened less effective, and hence the final state electron will have less kinetic energy.[25,26]

On the basis of the characterization results, it can be concluded that the IMC Pd_2Ga was accessed by the HTlc precursor approach in the form of structurally ordered nanoparticles. Their size well below 10 nm is much smaller than could be achieved by top-down approaches starting from bulk IMCs. However, the presence of minor amounts of elemental Pd particles or nanoparticulate intermetallic compounds with higher Pd content than in Pd_2Ga cannot be excluded, but no evidence was found by the methods applied. It is interesting to note that despite the large excess of Ga in the HTlc precursor the IMC formed at reduction temperatures up to 700 °C was always the 2:1 phase Pd_2Ga. This is probably due to the high stability of this phase and the nonability of this compound to form highly reactive hydrides which could reduce the Ga^{3+} in the vicinity. Furthermore, the presence of only oxidic Mg is proof for the successful parting of the Ga/Mg redox chemistry.

To finally test if not only the structural but also the excellent intrinsic catalytic properties of Pd−Ga IMCs reported in the literature[10,11] have been carried over to a nanostructured system, reference data of a well-defined bulk Pd_2Ga sample are needed for comparison. Such material is accessible by direct synthesis from the elements, which resulted in a single-phase sample after annealing at 900 °C (Figure 3). In contrast to the HTlc approach, the synthesis is thermodynamically controlled, and the process parameters can be varied in a relatively wide temperature and also a limited compositional range according to the binary phase diagram.[27]

Considering the dramatically different catalytic properties of Pd−Ga IMCs compared to elemental Pd, the observed selectivity of the samples in triple bond hydrogenation can be used as a sensitive test for the structural integrity of the IMC and the absence of residual elemental Pd. Catalytic tests in the semihydrogenation of acetylene were conducted at 200 °C and under atmospheric pressure for up to 25 h on stream. Figure 6 shows the conversion and selectivity of the melt-prepared bulk Pd_2Ga catalyst and the nanostructured HTlc-derived Pd_2Ga sample in comparison to a commercially available Pd/Al_2O_3 catalyst (5 wt %, Sigma Aldrich, 50−180 μm). Both IMC catalysts show a stable conversion of acetylene between 94 and 98% (Table 2). For the supported material, an activation of about 900% was observed in the first 23 h on stream, which cannot be due to incomplete reduction of the Pd species considering the pretreatment of the catalyst in hydrogen at 500 °C for 4 h. In contrast, the Pd/Al_2O_3 catalyst showed a strong deactivation from 100 to 20% conversion not reaching steady state conditions within 20 h on stream, which is most likely due to coke formation.[28] As expected, the selectivity of the pure Pd catalyst is much lower compared to the IMCs, and an ethylene selectivity of 20% was detected after 20 h. The highest selectivity of 74% was reached with the bulk Pd_2Ga catalyst. After the strong and slow activation, the $Pd_2Ga/MgO/MgGa_2O_4$ catalyst showed a

TABLE 2: Catalytic Properties of Pd−Ga-Based Materials Obtained at 200 °C[a]

catalysts	mass/mg	Pd/mg	TOS/h	X/%	S_{C2H4}/%	S_{C2H6}/%	S_{C4}/%	activity/mol_{C2H2}/mol_{Pd}
bulk Pd_2Ga	10	7.5	20	94	74	21	5	4.9
$Pd_2Ga/MgO/MgGa_2O_4$	0.047[b]	1.1×10^{-3}	24	98	70	26	5	28600.4
5 wt % Pd/Al_2O_3	0.1	5×10^{-3}	20	44	20	78	2	3430.7

[a] Other experimental conditions are given in the text. [b] Mass of precursor.

minimally lower selectivity of 70% after 23 h. The selectivity to higher hydrocarbons up to C4 was not higher than 5% for all catalysts.

In light of the similar catalytic properties of the two IMC catalysts under steady state conditions and the huge difference in particle sizes, it seems unlikely that the small difference in selectivity is related to a size effect. Other aspects also have to be considered when comparing bulk with nanoparticle catalysts. Porosity, interactions between nanoparticles, and support or absorptivity of substrate and reaction products may also serve as an explanation for these differences.[29] In addition, the presence of minor amounts of other Pd−Ga IMC with higher Pd content and probably lower selectivity might be responsible for the slightly lower selectivity observed here. Further studies of the supported Pd_2Ga nanoparticles are needed to solve these issues. Nevertheless, the novel supported Pd_2Ga nanocatalyst clearly out-performs the nanostructured metallic Pd reference sample in selectivity as well as in stability and the bulk reference sample in activity (Table 2). The activity per mass of Pd increased by a factor of 5700 compared to the bulk material. This renders the ex-HTlc $Pd_2Ga/MgO/MgGa_2O_4$ very promising for the application as a selective hydrogenation catalyst and reveals the high potential of our synthesis approach to achieve hydrogenation catalysts which resemble the selectivity of the model bulk material. Further optimization of this feasible synthesis route should enable the preparation of catalysts containing only Pd_2Ga as the catalytically active phase, possessing selectivities even closer to the bulk material.

Conclusion

Structurally ordered intermetallic compounds are a new promising class of catalytic materials, and Pd−Ga intermetallic compounds have shown excellent performance in the selective semihydrogenation substantially different from those of statistical alloys. Their intrinsic catalytic properties are related to the unique crystal and electronic structures. It was shown for the first time that these properties can be carried over from well-defined macroscopic model systems to nanostructured high-performance materials by a preparation method comprising coprecipitation of Pd, Ga, and Mg diluents in the form of a single-phase hydrotalcite-like precursor. This material can be decomposed in reducing atmosphere to yield Pd_2Ga nanoparticles (<10 nm) on a porous $MgO/MgGa_2O_4$ support. Due to the high dispersion and structural integrity of the intermetallic compound, the activity of the $Pd_2Ga/MgO/MgGa_2O_4$ catalyst is higher by a factor of more than 5700 compared to a bulk Pd_2Ga sample, while the selectivity and stability are still much higher than for a commercial elemental Pd reference catalyst. We suggest that this precursor method is generally promising for the synthesis of catalysts based on ordered Pd−X intermetallic compounds, X being elements forming hydrotalcite-like materials in their ionic form. Thereby, these materials, so far reported only in the form of model systems and not as high performance catalysts, are made available in the form of nanoparticles for comprehensive structural, electronic, and catalytic characterization.

Acknowledgment. The authors thank Gisela Lorenz, Edith Kitzelmann, Gisela Weinberg, and Gudrun Auffermann for the substantial help in the laboratory. Juri Grin is acknowledged for fruitful discussions.

References and Notes

(1) Wambach, J.; Baiker, A.; Wokaun, A. CO_2 Hydrogenation over Metal/Zirconia Catalysts. *Phys. Chem. Chem. Phys.* **1999**, *1*, 5071–5080.

(2) Borodziński, A.; Bond, G. C. Selective Hydrogenation of Ethyne in Ethene-Rich Streams on Palladium Catalysts, Part 2: Steady-State Kinetics and Effects of Palladium Particle Size, Carbon Monoxide, and Promoters. *Catal. Rev.* **2008**, *50*, 379–469.

(3) Thanh, C. N.; Didillon, B.; Sarrazin, P.; Cameron, C. U.S. Patent 6,054,409, 2000.

(4) Studt, F.; Abild-Pedersen, F.; Bligaard, T.; Sørensen, R. Z.; Christensen, C. H.; Nørskov, J. K. Identification of Non-Precious Metal Alloy Catalysts for Selective Hydrogenation of Acetylene. *Science* **2008**, *320*, 1320–1322.

(5) Studt, F.; Abild-Pedersen, F.; Bligaard, T.; Sørensen, R. Z.; Christensen, C. H.; Nørskov, J. K. On the Role of Surface Modifications of Palladium Catalysts in the Selective Hydrogenation of Acetylene. *Angew. Chem., Int. Ed.* **2008**, *47*, 9299–9302.

(6) Teschner, D.; Borsodi, J.; Wootsch, A.; Révay, Zs.; Hävecker, M.; Knop-Gericke, A.; David Jackson, S.; Schlögl, R. The Roles of Subsurface Carbon and Hydrogen in Palladium-Catalyzed Alkyne Hydrogenation. *Science* **2008**, *320*, 86–89.

(7) Teschner, D.; Révay, Zs.; Borsodi, J.; Hävecker, M.; Knop-Gericke, A.; Schlögl, R.; Milroy, D.; Jackson, S. D.; Torres, D.; Sautet, P. Understanding Palladium Hydrogenation Catalysts: When the Nature of the Reactive Molecule Controls the Nature of the Catalyst Active Phase. *Angew. Chem., Int. Ed.* **2008**, *47*, 9274–9278.

(8) Kovnir, K.; Armbrüster, M.; Teschner, D.; Venkov, T. V.; Jentoft, F. C.; Knop-Gericke, A.; Grin, Yu.; Schlögl, R. A new Approach to Well-defined, Stable and Site-isolated Catalysts. *Sci. Technol. Adv. Mater.* **2007**, *8*, 420–427.

(9) Kohlmann, H. *Metal Hydrides in Encyclopedia of Physical Science and Technology*, 3rd ed.; Academic Press: New York, 2002.

(10) Osswald, J.; Giedigkeit, R.; Jentoft, R. E.; Armbüster, M.; Girgsdies, F.; Kovnir, K.; Ressler, T.; Grin, Yu.; Schlögl, R. Palladium-Gallium Intermetallic Compounds for the Selective Hydrogenation of Acetylene Part II: Surface Characterization and Catalytic Performance. *J. Catal.* **2008**, *258*, 210–218.

(11) Osswald, J.; Kovnir, K.; Armbüster, M.; Giedigkeit, R.; Jentoft, R. E.; Wild, U.; Grin, Yu.; Schlögl, R. Palladium-Gallium Intermetallic Compounds for the Selective Hydrogenation of Acetylene Part I: Preparation and Structural Investigation under Reaction Conditions. *J. Catal.* **2008**, *258*, 219–227.

(12) Kovnir, K.; Osswald, J.; Armbrüster, M.; Teschner, D.; Weinberg, G.; Wild, U.; Knop-Gericke, A.; Ressler, T.; Grin, Yu.; Schlögl, R. Etching of the Intermetallic Compounds PdGa and Pd_3Ga_7: An Effective Way to Increase Catalytic Activity. *J. Catal.* **2009**, *264*, 93–103.

(13) Komatsu, T.; Inaba, K.; Uezono, T.; Onda, A.; Yashima, T. Nano-size Particles of Palladium Intermetallic Compounds as Catalysts for Oxidative Acetoxylation. *Appl. Catal., A* **2003**, *251*, 315–326.

(14) Penner, S.; Lorenz, H.; Jochum, W.; Stöger-Pollach, M.; Wang, D.; Rameshan, C.; Klötzer, B. Pd/Ga_2O_3 Methanol Steam Reforming Catalysts: Part I. Morphology, Composition and Structural Aspects. *Appl. Catal., A* **2009**, *358*, 193–202.

(15) Lorenz, H.; Penner, S.; Jochum, W.; Rameshan, C.; Klötzer, B. Pd/Ga_2O_3 Methanol Steam Reforming Catalysts: Part II. Catalytic Selectivity. *Appl. Catal., A* **2009**, *358*, 203–210.

(16) Armbrüster M.; Schmidt M.; Kovnir K.; Friedrich M.; Weinhold K.; Grin Yu.; Schlögl R. Preparation of Intermetallic Compounds via Gas Phase and Nanoparticle Syntheses. EP07021904A1. European Patent Application, 2007.

(17) Cavani, F.; Trifirò, F.; Vaccari, A. Hydrotalcite-type Anionic Clays: Preparation, Properties and Applications. *Catal. Today* **1991**, *11*, 173–301.

(18) Basile, F.; Vaccari, A. *Layered Double Hydroxides-Present and Future*; Rives, V., Ed.; Nova Science Publishers: New York, 2001.

(19) Behrens, M.; Kasatkin, I.; Kühl, S.; Weinberg, G. Phase-Pure Cu, Zn, Al Hydrotalcite-like Materials as Precursors for Copper rich Cu/ZnO/Al_2O_3 Catalysts. *Chem. Mater.* **2010**, *22*, 386–397.

(20) De Roy, A. Lamellar Double Hydroxides. Mol. Cryst. *Liq. Cryst.* **1998**, *311*, 173–193.

(21) Gorodetskii, V. V.; Sametova, A. A.; Matveev, A. V.; Tapilin, V. M. From Single Crystals to Supported Nanoparticles in Experimental and Theoretical Studies of H_2 Oxidation over Platinum Metals (Pt, Pd): Intermediates, Surface Waves and Spillover. *Catal. Today* **2009**, *144*, 219–234.

(22) Aramendía, M. A.; Avíles, Y.; Borau, V.; Luque, J. M.; Marinas, J. M.; Ruiz, J. R.; Urbano, F. J. Thermal Decomposition of Mg/Al and Mg/Ga Layered-double Hydroxides: A Spectroscopic Study. *J. Mater. Chem.* **1999**, *9*, 1603–1607.

(23) Schön, G. Auger and Direct Electron Spectra in X-ray Photoelectron Studies of Zinc, Zinc Oxide, Gallium and Gallium Oxide. *J. Electron Spectrosc. Relat. Phenom.* **1973**, *2*, 75–86.

(24) Kovnir, K.; Teschner, D.; Armbrüster, M.; Schnörch, P.; Hävecker, M.; Knop-Gericke, A.; Grin, Yu.; Schlögl, R. Pinning the Catalytic Centre: A new Concept for Catalysts Development. *BESSY Highlights* **2007**, *2008*, 22–23.

(25) Zhang, L.; Persaud, R.; Madey, T. E. Ultrathin Metal Films on a Metal Oxide Surface: Growth of Au on TiO_2 (110). *Phys. Rev. B* **1997**, *56*, 10549–10557.

(26) Oberli, L.; Monot, R.; Mathieu, H. J.; Landolt, D.; Buttet, J. Auger and X-ray Photoelectron Spectroscopy of small Au Particles. *Surf. Sci.* **1981**, *106*, 301–307.

(27) Okamoto, H. Ga-Pd (Gallium-Palladium). *J. Phase Equilib. Diffus.* **2008**, *29*, 466–467.

(28) Ahn, Y.; Lee, J. H.; Kim, S. K.; Moon, S. H. Three-stage deactivation of Pd/SiO_2 and $Pd-Ag/SiO_2$ catalysts during the selective hydrogenation of acetyleneAppl. *Catal. A* **2009**, *360*, 38–42.

(29) Bond, G. C. Supported Metal Catalysts: Some unsolved Problems. *Chem. Soc. Rev.* **1991**, *20*, 441–475.

(30) Kovnir, K.; Schmidt, M.; Waurisch, C.; Armbrüster, M.; Prots, Yu.; Grin, Yu. Refinement of the Crystal Structure of Dipalladium Gallium, Pd_2Ga. *Z. Kristallogr. - New Cryst. Struct.* **2008**, *223*, 7–8.

JP109226R